4. STRATOSPHERIC OZONE

—M. Weber, W. Steinbrecht, C. Arosio, R. van der A, S. M. Frith, J. Anderson, L. M. Ciasto, M. Coldewey-Egbers, S. Davis, D. Degenstein, V. E. Fioletov, L. Froidevaux, D. Loyola, A. Rozanov, V. Sofieva, K. Tourpali, R. Wang, T. Warnock, and J. D. Wild

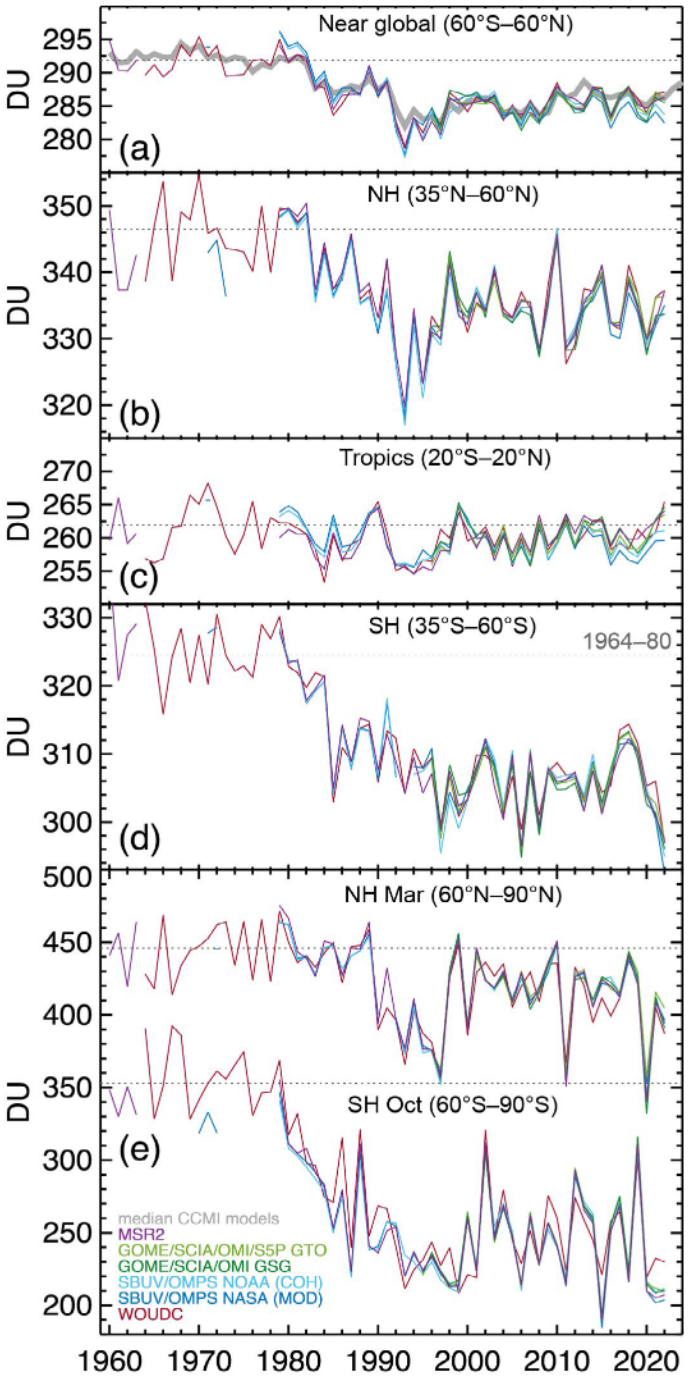

Stratospheric ozone protects Earth's biosphere from harmful ultraviolet (UV) radiation. The phase-out of ozone-depleting substances (ODSs) mandated by the Montreal Protocol and its Amendments (section 2g2) stopped the continuous decline of stratospheric ozone observed before the mid-1990s (Fig. 2.63). Some regions indicate a slow recovery attributed to the ODS decline, most notably the upper stratosphere (Figs. 2.64a–c; WMO 2022; Arosio et al. 2019; Sofieva, et al. 2021; Coldewey-Egbers et al. 2022; Godin-Beekmann et al. 2022; Weber et al. 2022). The rate and the sign of long-term ozone changes depend on changes in chemical composition (e.g., ODSs) and stratospheric circulation, which vary by region and altitude and are partly due to increasing long-lived greenhouse gases (LLGHGs). Both stratospheric cooling due to LLGHG and ODS decline are expected to reduce stratospheric ozone loss outside the polar region (Stolarski et al. 2015).

Relative to a base period of 1998–2008, 2022 annual mean total ozone anomalies poleward of 30° latitude in each hemisphere were mostly negative, while positive anomalies were observed at lower latitudes and in the tropics (Plate 2.1y). These anomalies are related to the La Niña (https://psl.noaa.gov/enso/mei/) and the mostly westerly shear phase of the quasi-biennial oscillation (above 30 hPa) in 2022. The associated weakening of the tropical upwelling and Brewer-Dobson circulation (BDC) leads to higher ozone in the tropics and reduced ozone transport into high latitudes and, at the same time, decreases polar stratospheric temperatures in winter/spring, thereby enhancing spring polar ozone losses (Domeisen et al. 2019).

Fig. 2.63. Time series of annual mean total column ozone (DU) in (a)–(d) four zonal bands and (e) polar (60°–90°) total column ozone in Mar (Northern Hemisphere, NH) and Oct (Southern Hemisphere, SH), the months when polar ozone losses usually are largest. Data are from World Ozone and Ultraviolet Radiation Data Centre (WOUDC) ground-based measurements combining Brewer, Dobson, Système D'Analyse par Observations Zénithales (SAOZ), and filter spectrometer data (red; Fioletov et al. 2002, 2008); the BUV/SBUV/SBUV2/OMPS merged products from NASA (V8.7; dark blue; Frith et al. 2014, 2017), and NOAA (SBUV V8.6, OMPS V4r1; light blue; Wild and Long pers. comm., 2019); the GOME/SCIAMACHY/GOME-2/OMPS/(TROPOMI) products GSG from University of Bremen (dark green; Weber et al. 2022), and GTO from the ESA/DLR dataset (light green; Coldewey-Egbers et al. 2015; Garane et al. 2018). MSR2 (purple) assimilates nearly all ozone datasets after corrections based on the ground-based data (van der A et al. 2015). All datasets have been bias-corrected by subtracting averages for the reference period 1998–2008 and adding back the mean of these averages. The dotted gray lines in each panel show the average ozone level for 1964–80 calculated from the WOUDC data. The thick gray lines in (a) show the median ozone level from CCMI-1 ref C2 model runs (SPARC/IO3C/GAW 2019). Most of the observational data for 2022 are preliminary.

The variability in lower stratospheric ozone is largest in winter/spring in both hemispheres, which drives the annual mean variations, as seen in Figs. 2.63 and 2.64.

The various annual mean time series of total ozone (Fig. 2.63) convey the same picture as observed in Plate 2.1y. At midlatitudes (35°–60°) in both hemispheres (Figs. 2.63b,d), the annual mean total ozone in 2022 was close to the long-term mean (1998–2008) in the Northern Hemisphere and at the lower end of values during the last decade in the Southern Hemisphere (SH). Particularly striking are the very low 2022 values in the SH, which are close to the all-time low of the previous sixty years. Very low stratospheric ozone is also evident at the 50-hPa level (Fig. 2.64f). Contrastingly, 50-hPa ozone and total columns from selected datasets (WOUDC, GSG, GTO) are close to the maximum observed during the last two decades (Figs. 2.63c, 2.64e).

In addition to the effect of La Niña, the underwater volcanic eruption from Hunga Tonga–Hunga Ha‘pai (HTHH) in January 2022 may have contributed to this low annual mean SH ozone in 2022. HTHH injected large quantities of aerosols and water vapor into the stratosphere that reduced stratospheric temperatures and modified chemical reaction cycles (sections 2g5, 2g3; Sidebar 2.2; Bourassa et al. 2022; Millán et al. 2022; Vömel et al. 2022). The weakening of the residual BDC in the SH caused by HTHH contributed to the drop in SH middle lower stratospheric and column ozone in 2022 (Coy et al. 2022; Wang et al. 2022). The transport of enhanced aerosol levels into the polar region, and circulation-driven lower polar temperatures may have caused additional Antarctic ozone losses (Wang et al. 2022). While the anomalously weak planetary wave activity in austral spring was the main cause of the deeper Antarctic ozone holes during the last three years (section 6i), recent studies suggest that Australian wildfires in December 2019, volcanic events of La Soufrière in April 2021, and HTHH in early 2022 contributed to the low ozone levels in the lower stratosphere at southern midlatitudes

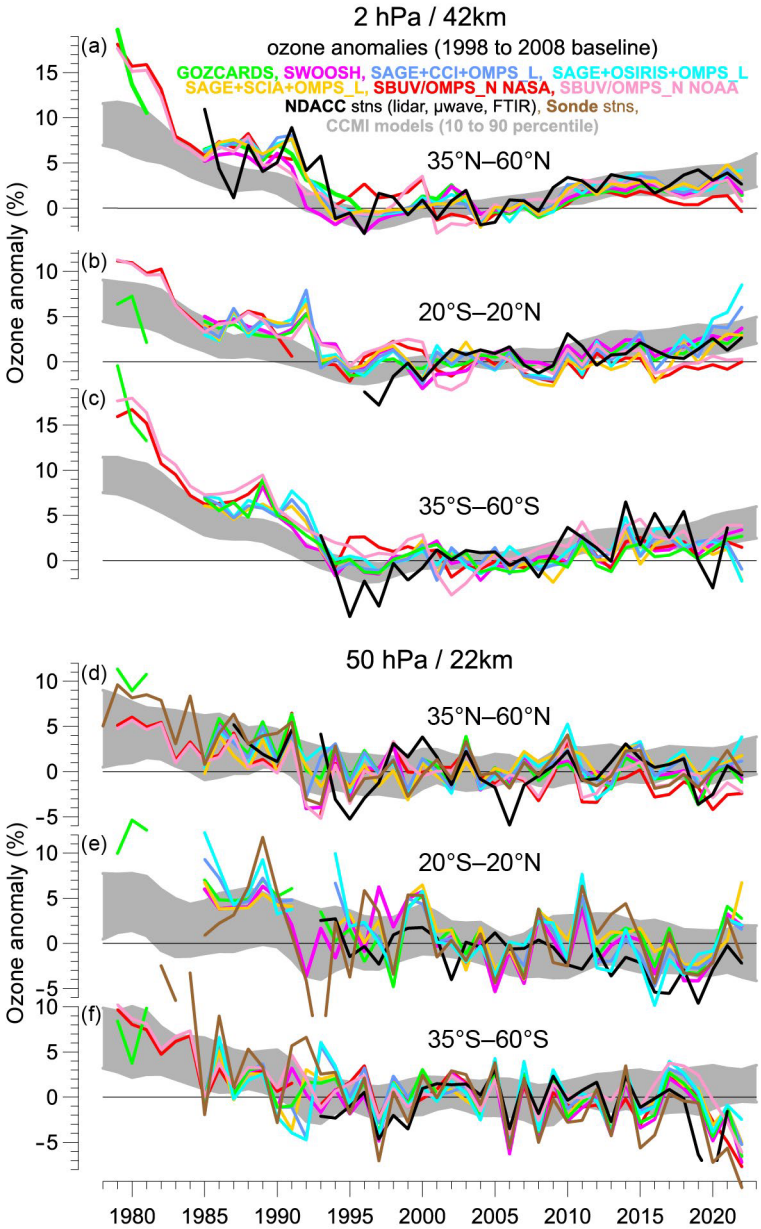

Fig. 2.64. Annual mean anomalies of ozone in (a)–(c) the upper stratosphere near 42-km altitude or 2-hPa pressure, and (d)–(f) in the lower stratosphere near 22 km or 50-hPa pressure for three zonal bands: (a),(d) 35°N–60°N, (b),(e) 20°S–20°N (tropics), and (c),(f) 35°S–60°S. Anomalies are with respect to the 1998–2008 base period. Colored lines are long-term records obtained by merging different limb (GOZCARDS, SWOOSH, SAGE+CCI+OMPS-L, SAGE+SCIAMACHY+OMPS-L) or nadir-viewing (SBUV, OMPS-N) satellite instruments. The nadir-viewing instruments have much coarser altitude resolution than the limb-viewing instruments. This can cause differences in some years, especially at 50 hPa. The black line is from merging ground-based ozone records at seven Network for the Detection of Atmospheric Composition Changes (NDACC) stations employing differential absorption lidars and microwave radiometers. See Steinbrecht et al. (2017), WMO (2018), and Arosio et al. (2018) for details on the various datasets. Gray shaded area shows the range of chemistry-climate model simulations from CCMI-1 refC2 (SPARC/IO3C/GAW 2019). Ozone data for 2022 are not yet complete for all instruments and are still preliminary.

(Figs. 2.63d, 2.64f) and deeper Antarctic ozone holes (Figs. 2.64f; Rieger et al. 2021; Ansmann et al. 2022; Yook et al. 2022; Strahan et al. 2022; Wang et al. 2022, Solomon et al. 2023).

Ozone profile data (Fig. 2.64f) confirm the low total ozone at southern midlatitudes. Apart from this, Fig. 2.64 shows ozone values in 2022 that are generally consistent with expectations from model simulations of the Phase 1 Chemistry Climate Model Initiative (CCMI) based on current scenarios of ODS and greenhouse gas changes (thick gray line in Fig. 2.63a; shaded area in Fig. 2.64; SPARC/IO3C/GAW 2019): 1) slow but noticeable recovery of ozone in the upper stratosphere over the last 20 years (WMO 2022; Godin-Beekmann et al. 2022), with observations in recent years closer to the lower end of the model simulations; and 2) little or no recovery of ozone in the lower stratosphere, with recent midlatitude observations at the lower end of the simulations (Ball et al. 2020; Thompson et al. 2021; Godin-Beekmann et al. 2022; WMO 2022).

5. STRATOSPHERIC WATER VAPOR

—S. M. Davis, K. H. Rosenlof, D. F. Hurst, H. Vömel, and R. Stauffer

Normally, water vapor (WV) entering the stratosphere is regulated by temperatures in the tropical tropopause layer (TTL; ~14 km–19 km), with higher WV concentrations occurring when TTL temperatures are higher. However, the 14–15 January 2022 eruptions of the Hunga Tonga–Hunga Ha‘apai (HTHH) submarine volcano (20.54°S, 175.4°W) injected an amount of water vapor (~50 Tg–150 Tg) into the stratosphere that is unprecedented in the satellite record and represents upwards of 10% of the entire stratospheric burden of WV (Carr et al. 2022; Khaykin et al. 2022; Legras et al. 2022; Millán et al. 2022; Proud et al. 2022; Vömel et al. 2022; see also Sidebar 2.2). By being injected at between approximately 26 km and 34 km, WV associated with the HTHH eruption bypassed the TTL “cold trap” and resulted in a dramatic perturbation to WV and other stratospheric species (e.g., ozone, section 2g4) that will likely persist for years.

This direct injection of WV into the stratosphere by HTHH is evident in the so-called “tropical tape recorder” (Mote et al. 1996) plot (Fig. 2.65a). The WV anomaly appears suddenly in early 2022 between roughly 40 hPa and 10 hPa and then ascends through the stratosphere as part of the meridional overturning circulation. Within the tropical latitude band (15°S–15°N), this unprecedented zonal-mean monthly-mean anomaly (relative to the 2004–21 mean) peaked at 6.4 ppm (parts per million, i.e., μmol mol^{-1}) above the climatological normal of 4.1 ppm

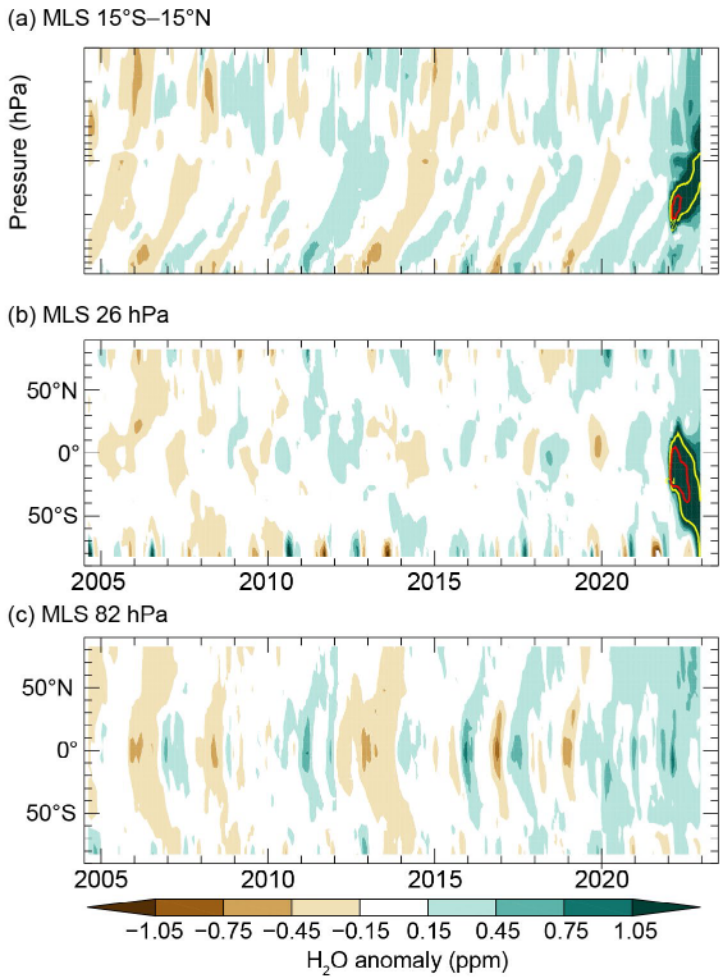

Fig. 2.65. (a) Latitude–time contour of tropical (15°S–15°N) lower-stratospheric water vapor (WV) anomalies, with the +2 ppm and +4 ppm values shown as yellow and red contour lines, respectively. (b),(c) Latitude–time contour of WV anomalies at (b) 26 hPa and (c) 82 hPa, respectively. All panels are based on version 5.01 Aura MLS data, which has collected near-global (82°S–82°N) measurements since Aug 2004. Anomalies are differences from the mean 2004–21 WV mixing ratios (ppm) for each month. (a) shows the unprecedented injection of water vapor directly into the stratosphere by the Hunga Tonga–Hunga Ha‘apai eruption. (b) shows the southward propagation of the plume at 26 hPa, while (c) shows a more general propagation of tropical lower-stratospheric WV anomalies to higher latitudes in both hemispheres as well as the influences of dehydrated air masses from the Antarctic polar vortex as they are transported toward the Southern Hemisphere midlatitudes at the end of each year. Tick marks denote the beginning of each year.